Cardiovascular Toxicology (2019) 19:297–305
https://doi.org/10.1007/s12012-019-09511-2

Micheliolide Protects Against Doxorubicin-Induced Cardiotoxicity in Mice by Regulating PI3K/Akt/NF-kB Signaling Pathway

Ashkan Kalantary-Charvadeh[1,4] · Davoud Sanajou[1] · Mohsen Hemmati-Dinarvand[2] · Yasser Marandi[3] · Mehran Khojastehfard[1] · Hamed Hajipour[5] · Mehran Mesgari-Abbasi[6] · Leila Roshangar[7] · Saeed Nazari Soltan Ahmad[1]

Published online: 5 March 2019

Abstract

Micheliolide (MCL) is a naturally derived anti-inflammatory agent. In the present investigation, we examined the protective potential of MCL against doxorubicin (DOX)-induced cardiotoxicity in mice. Mice were injected with a single 15-mg/kg intraperitoneal dose of DOX at day 1 and the study groups received daily 12.5, 25, and 50 mg/kg doses of MCL for 7 days. Cardiac histopathology, cardiac function, serum markers of cardiac injury, and tissue markers of inflammation, and oxidative stress were examined. MCL decreased serum levels of creatinine kinase MB (CK-MB) and cardiac troponin I (cTnI) levels, ameliorated cardiac tissue architecture, and improved cardiac stroke volume. Apart from reducing the activities of NF-kB p65 subunit, MCL attenuated the cardiac levels of PI3K, phosphorylated (p)-Akt, p-Bad, and caspase-3 levels and simultaneously elevated p-PTEN levels. While the gene expressions of tumor necrosis factor alpha (TNF-α) and interleukin 1 beta (IL-1β) were decreased, the tissue activities of superoxide dismutase (SOD) as well as gene expressions of heme oxygenase-1 (HO-1) and NAD(P)H quinone dehydrogenase-1 (NQO1) were increased after treatment with MCL. Furthermore, tissue levels of malondialdehyde (MDA) were also decreased. Collectively, these findings point to the protective effects of MCL against DOX-induced cardiotoxicity by regulating PI3K/Akt/NF-kB signaling pathway in mice.

Keywords Akt · Doxorubicin-induced cardiotoxicity · Micheliolide · NF-kB · PI3K

Introduction

Doxorubicin, an anthracycline antineoplastic agent, is used for the treatment of solid tumors as well as hematopoietic malignancies [1]. While lower doses of doxorubicin are relatively safe, it has been found that 5% of patients receiving a cumulative dose of more than 300 mg/m^2 doxorubicin develop congestive heart failure after a median follow-up period of 6.3 years [2]. Generally the cumulative dose of doxorubicin rarely exceeds 300 mg/m^2; however, cardiotoxicity could still develop at lower doses and histopathologic derangements have been observed in myocardial biopsy specimens from individuals receiving as little as 240 mg/m^2 of doxorubicin [3]. Liposomal formulations of doxorubicin evoke less cardiac side effects while having the same anti-cancer activities as the conventional preparations [4]. A myriad of detrimental effects supervene in the cardiac tissues after the administration of the high doses of doxorubicin including the production of reactive oxygen species (ROS), mitochondrial bio-energetic failure, endoplasmic

Handling Editor: Dipak K Dube

✉ Saeed Nazari Soltan Ahmad
saeednazari0078@gmail.com

1 Department of Biochemistry, Faculty of Medicine, Tabriz University of Medical Sciences, Golgasht Avenue, Tabriz 57191-58875, Iran

2 Department of Biochemistry, Faculty of Medicine, Shiraz University of Medical Sciences, Shiraz, Iran

3 Department of Biochemistry, Faculty of Medicine, Hamedan University of Medical Sciences, Hamedan, Iran

4 Student Research Committee, Tabriz University of Medical Sciences, Tabriz, Iran

5 Department of Reproductive Biology, Faculty of Advanced Medical Sciences, Tabriz University of Medical Sciences, Tabriz, Iran

6 Drug Applied Research Center, Tabriz University of Medical Sciences, Tabriz, Iran

7 Stem Cell Research Center, Tabriz University of Medical Sciences, Tabriz, Iran

reticulum stress as well as impaired calcium homeostasis, and NF-kB ultra-activation with associated hyperinflammation and apoptosis [5]. To date, several agents with antioxidant and anti-inflammatory properties like vitamin E, L-carnitine, coenzyme Q, glutathione, and *N*-acetylcysteine have been examined in experimental and clinical investigations with promising, albeit disparate, outcomes and none have been validated in the large clinical trials; therefore, present interventions are limited to the treatment guidelines set for the heart failure patients [6].

Micheliolide (MCL) is a plant-derived guaianolide sesquiterpene lactone with notable anti-inflammatory properties, shown to be effective against experimental models of acute myelogenous leukemia and colorectal cancer [7]. Indeed, beneficial therapeutic effects of MCL in lipopolysaccharide-induced neuroinflammation and mycobacterium tuberculosis-induced immune response through alleviation of oxidative stress and suppression of inflammation by modulating NF-κB signaling pathway have been studied [8, 9]. Based on these promising findings, we postulated that MCL could potentially exert protective effects against doxorubicin-induced cardiotoxic mice and devised the current investigation to test our hypothesis.

Methods

Materials

Micheliolide and doxorubicin were purchased from ChemFaces (Wuhan, China) and Pfizer (New York City, New York, USA), respectively.

Experimental Animals and Protocol

Thirty-six male C57BL/6 mice (8–10 weeks old, 20–22 g) were obtained from Pasteur Institute of Iran (Tehran, Iran). All studies were conducted under strict adherence to the principles of laboratory animal care (NIH publication no. 85–23, revised 1985) and the study protocol was mandated by the Ethics Committee for Animal Studies, Tabriz University of Medical Sciences (Ethical code: IR.TBZMED.REC.1397.128). Mice were divided into 6 groups of 6 per each. The sham group deemed to be the healthy controls; the second group received a single dose of doxorubicin (15 mg/kg, intraperitoneally) at day 1. The groups 3 to 5, in addition to doxorubicin, were injected daily doses of 12.5 mg/kg, 25 mg/kg, and 50 mg/kg micheliolide, respectively, dissolved in normal saline [10]. The last group received only 50 mg/kg of MCL. Because of optimal mimic of acute doxorubicin toxicity, animals received the treatment for 7 days [11] and then were anesthetized by an intraperitoneal injection of 50 mg/kg ketamine and 1 mg/kg midazolam. Blood sampling was done by cardiac puncture and then tissue samples were extracted for further analysis.

Assessment of Oxidative Stress Indices in Cardiac Tissues

Heart tissues were homogenized in ice-cold phosphate-buffered saline (PBS) solution (0.1 M, PH 7.4). The homogenates were centrifuged at 5000×*g* for 15 min at 4 °C and the obtained supernatant was used for the assessment of the total protein content, superoxide dismutase (SOD) and glutathione peroxidase (GPX) activities, and malondialdehyde (MDA) concentrations. Total protein content was evaluated by the Lowry method. SOD and GPX activities and MDA levels were measured by using the commercial colorimetric assay kits (Biorex Fars, Shiraz, Iran) according to the manufacturer's instructions.

Cardiac Histopathologic Assessment

Cardiac tissue specimens were fixed in 10% neutral-buffered formalin (NBF) and processed for paraffin sections of five μm thickness. Sections were stained with Hematoxylin and Eosin (H&E) and examined under a light microscope (PW108, Proway, China) [12].

Real Time-qPCR

Total RNA was isolated by using a Total RNA extraction kit (Macherey Nagel, Düren, Germany) and was transcribed into complementary cDNA by using the first-strand cDNA synthesis kit (Thermo Fisher Scientific, Waltham, MA). RT-qPCR was performed by using the primers listed in Table 1. The relative expressions of the genes were calculated via the $2^{-\Delta\Delta C_T}$ equation.

Table 1 List of primers and their respective sequences

Primer name	Forward sequence	Reverse sequence
TNF-α	GCCTATGTCTCAGCCTCTTCTC	GGCCATTTGGGAACTTCTCATC
IL-1β	TCCCATTAGACAACTGCACTAC	GCTCATGGAGAATATCACTTGTTG
HO-1	CAACATTGAGCTGTTTGAGGAG	GTGTCTGGGATGAGCTAGTG
NQO-1	ACCTGGTGATATTTCAGTTCCC	AGTGGTGATAGAAAGCAAGGTC
GAPDH	TGAACGGATTTGGCCGTATTG	CTTGACTGTGCCGTTGAATTTG

Serum Biochemical and Immunochemical Analyses

Serum heart-type fatty acid-binding protein (H-FABP) was measured by using an enzyme-linked immunosorbent assay (ELISA) kit (Dldevelop, Wuxi, China). Similarly, glycogen phosphorylase isoenzyme BB (GP-BB) was assayed by using a commercially ELISA kit (Creative Diagnostics, Shirley, NY). Creatine kinase isoform MB (CK-MB) was quantitated by using a commercial colorimetric assay kit (Pars Azmoon, Tehran, Iran). A particle-enhanced turbidimetric immunoassay (PETIA) kit was adopted for the measurement of the serum myoglobin (Weldon Biotech, Haridwar, India). Finally, serum cardiac troponin I (cTnI) was measured with a fluorometric immunoassay (FLIA) kit (BioMérieux, Marcy-l'Étoile, France).

Western Blotting

Fifty mg of the cardiac tissues of each mouse was cut and pooled with respect to the study groups. Tissues were homogenized by radioimmunoprecipitation assay (RIPA) buffer (Santa Cruz). Total protein content in each sample was measured by the Bradford method and the equal amounts of 20 µg protein were electrophoresed on the sodium dodecyl sulfate polyacrylamide gel electrophoresis (SDS-PAGE). After blotting the bands on the PVDF membranes (Cleaver Scientific, Warwickshire, UK), the blocking step was carried out by using the 5% skimmed milk and then blotted membranes were incubated with the primary antibodies against phosphoinositide 3-kinase (PI3K) (Santa Cruz, sc-1637), phosphorylated phosphatase and tensin homolog (p-PTEN) (Santa Cruz, sc-377573), phosphorylated p-Akt (Santa Cruz, sc-514032), Bad (Santa Cruz, sc-8044), p-Bad (Santa Cruz, sc-271963), and caspase-3 (Santa Cruz, sc-7272) antibodies overnight at 4 °C. Then, secondary horse radish peroxidase (HRP)-conjugated antibodies (Santa Cruz, sc-516102) were applied and Western Blotting Luminol Reagent (Santa Cruz) was implemented for the final visualization step. The loading control was β-actin (Santa Cruz, sc-47778). The recorded bands on the radiographic films were measured semi-quantitatively. The intensity of each band was normalized by the intensity of the correspondent β-actin band. The relative intensities were reported as the fold change over the values obtained for normal control mice. Calculations were carried out by using the ImageJ analysis software (version 1.41).

Assessment of Cardiac Function

Manual measurement of the coronary (Qe) and aortic (Qa) flow rates (ml/min) were carried out during the working heart mode. The aortic pressure (PAO, mmHg) was quantitated by using a Viggo-Spectramed pressure transducer connected to the sidearm of the aortic cannula. Moreover, the peak systolic pressure (PSP) and heart rate (HR) values were recorded during the measurements. To evaluate cardiac function, the values for cardiac output and stroke volume were calculated as follows: cardiac output (CO) (ml/min) = (Qe + Qa); stroke volume (SV) (ml/min) = (CO/HR) [13].

NF-kB Activity Assay

NF-kB (p65) Transcription Factor Assay Kit (Cayman Chemical, Ann Arbor, MI) was used for the measurement of the NF-kB activities in the cardiac tissues. Briefly, the nuclear fractions of tissue lysates were extracted by using a nuclear extraction kit (Cayman Chemical) and their protein content were assayed by using the Bradford method. Equal amounts of 20 µg protein were loaded into each microplate well pre-coated with the consensus dsDNA capable of binding to the phosphorylated p65 subunit of the NF-kB. Then, anti-phosphorylated p65 primary antibody, HRP-conjugated secondary antibody, and chromogen substrate solutions were added sequentially. The light absorbance of the wells was read at 450 nm and reported as the estimate of the NF-kB activities.

Statistical Analyses

Values are expressed as mean ± standard deviation (SD). Analysis of data was conducted by using the SPSS, version 18. Kruskal–Wallis (KW) followed by Dunn–Bonferroni post hoc test was used to assess the statistical significance between the treatment groups. Values of $P < 0.05$ were considered significant.

Results

Cardiac Inflammation and Oxidative Stress

The gene expression of the salient inflammatory cytokines, i.e., TNF-α and IL-1β, were increased in the cardiac tissues of the DOX-treated mice as compared to sham group ($P < 0.01$), and 50 mg/kg MCL significantly reduced the expressions of these inflammatory mediators ($P < 0.05$) (Fig. 1a, b). Moreover, increased activities of the NF-kB p65 subunit were noted in the cardiac tissues of the DOX group compared with sham mice ($P < 0.01$). While 12.5 and 25 mg/kg MCL had no statistically significant effects on the NF-kB activities, 50 mg/kg dose of the drug reduced its activities in the cardiac tissues (Fig. 1e).

Elevated levels of MDA in the heart tissues of DOX mice were observed as compared to sham mice ($P < 0.05$); furthermore, the activities of both SOD and GPX were noticed to be increased in the cardiac tissues

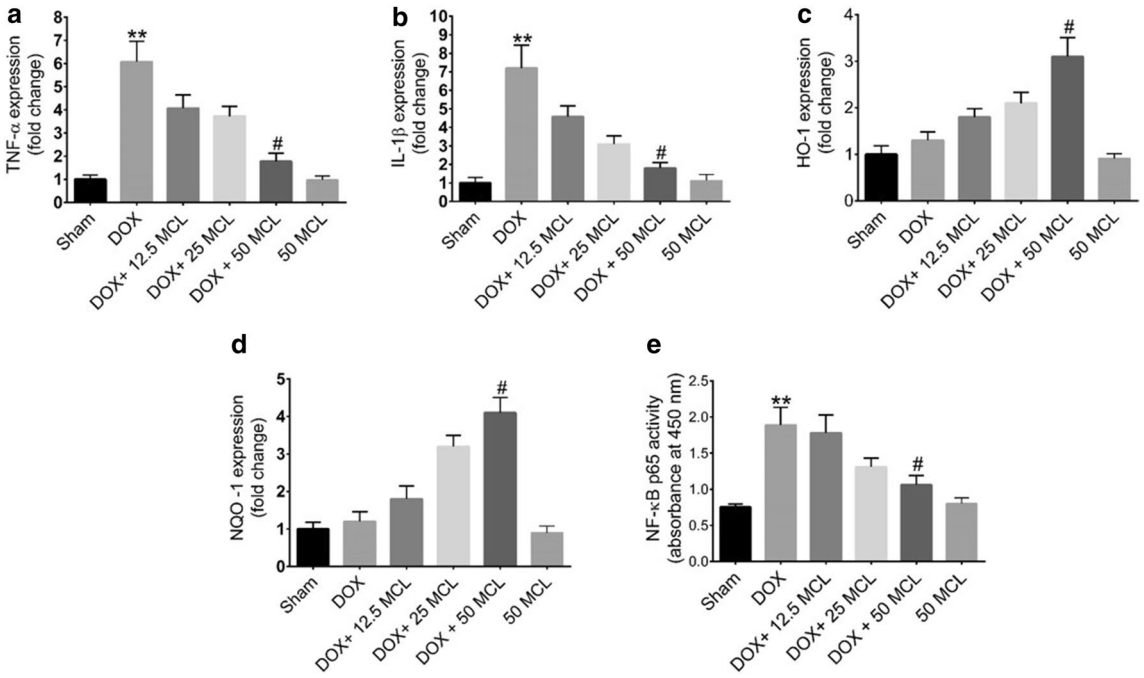

Fig. 1 Effects of MCL on cardiac expressions of TNF-α (**a**), IL-1β (**b**), HO-1 (**c**), and NQO-1 (**d**) and cardiac activities of NF-κB p65 (**e**) in DOX-induced cardiotoxic mice. Gene expressions were evaluated by RT-qPCR. *MCL* micheliolide, *TNF-α* tumor necrosis factor alpha, *IL-1β* interleukin 1beta, *DOX* doxorubicin. Sham ($N=6$), healthy control mice; DOX ($N=6$), DOX-induced cardiotoxic control mice; DOX + 12.5 MCL ($N=6$), DOX-induced cardiotoxic mice treated with 12.5 mg/kg MCL; DOX + 25 MCL ($N=6$), DOX-induced cardiotoxic mice treated with 25 mg/kg MCL; DOX + 50 MCL ($N=6$), DOX-induced cardiotoxic mice treated with 50 mg/kg MCL; MCL 50 ($N=6$), healthy mice receiving 50 mg/kg MCL. $^{*}p<0.05$, $^{**}p<0.01$, $^{***}p<0.001$ versus Sham. $^{\#}p<0.05$, $^{\#\#}p<0.01$, $^{\#\#\#}p<0.001$ versus DOX

of DOX-treated animals compared with sham group ($P<0.05$). 50 mg/kg MCL reduced cardiac MDA levels from 121.1 ± 11.4 nmol/g tissue in control DOX mice to 64.3 ± 7.8 nmol/g tissue ($P<0.05$) and at the same time the activities of SOD in DOX mice were increased from 70.5 ± 6.7 U/g tissue to 94.5 ± 4.1 U/g tissue ($P<0.05$). 50 mg/kg MCL reduced cardiac MDA levels from 121.1 ± 11.4 nmol/g tissue in control DOX mice to 64.3 ± 7.8 nmol/g tissue ($P<0.05$) and at the same time it elevated the activities of SOD from 70.5 ± 6.7 U/g tissue in control DOX mice to 94.5 ± 4.1 U/g tissue ($P<0.05$). While the cardiac levels of GPX were increased after treatment with MCL in DOX mice, it was recognized to be statistically insignificant at any MCL dose (Table 2). Similarly, the gene expressions of the anti-oxidant proteins HO-1 and NQO-1 revealed to be elevated in DOX mice receiving 50 mg/kg MCL ($P<0.05$) (Fig. 1c, d).

Table 2 Markers of oxidative stress in cardiac tissues

	Sham ($N=6$)	DOX ($N=6$)	DOX + 12.5 MCL ($N=6$)	DOX + 25 MCL ($N=6$)	DOX + 50 MCL ($N=6$)	50 MCL ($N=6$)
MDA (nmol/g tissue)	43.7 ± 4.2	126.1 ± 11.4[a]	105.5 ± 9.8[a]	87.9 ± 10.2[a]	64.3 ± 7.8[a,b]	40.1 ± 5.6
SOD (U/g tissue)	55.8 ± 4.4	70.5 ± 6.7[a]	79.3 ± 4.3[a]	86.1 ± 5.2[a]	94.5 ± 4.1[a,b]	57.4 ± 4.9
GPX (U/g tissue)	6.3 ± 1.2	8.5 ± 1.1[a]	9.1 ± 1.3[a]	10.4 ± 1.6[a]	11.7 ± 1.5[a]	5.7 ± 1.3

Sham, healthy control mice; DOX, DOX-induced cardiotoxic control mice; DOX + 12.5 MCL, DOX-induced cardiotoxic mice treated with 12.5 mg/kg MCL; DOX + 25 MCL, DOX-induced cardiotoxic mice treated with 25 mg/kg MCL; DOX + 50 MCL, DOX-induced cardiotoxic mice treated with 50 mg/kg MCL; MCL 50 ($N=6$), healthy mice receiving 50 mg/kg MCL. Values are presented as mean ± SD

DOX doxorubicin, *GPX* glutathione peroxidase, *MCL* micheliolide, *MDA* malondialdehyde, *SOD* superoxide dismutase

[a] $P<0.05$ versus Sham

[b] $P<0.05$ versus DOX

Serum Indices of Cardiac Injury

Serum myoglobin, H-FABP, GP-BB, CK-MB, and cTnI levels were identified to be significantly elevated in DOX mice ($P < 0.05$). Myoglobin, H-FABP, and GP-BB levels remained almost unchanged after treatment with any dose of the MCL (Table 3). While 50 mg/kg MCL attenuated increased activities of CK-MB in DOX-treated mice by 36.69%, it reduced the levels of cTnI from 6.77 ± 1.18 to 4.66 ± 0.83 ng/ml in DOX-treated mice ($P < 0.05$) (Table 3).

Cardiac Histopathology

Hearts from the normal control and 50 mg/kg MCL group mice demonstrated normal histoarchitecture (Fig. 2a, f). Examination of cardiac tissues from DOX control mice and DOX mice treated with 12.5 mg/kg MCL revealed marked histological alterations in the form of myofibrillar loss, inflammatory cell infiltration, cell vacuolization, and necrosis (Fig. 2b, c). Treating intoxicated mice with 25 mg/kg MCL distinctly improved cardiomyocyte damage (Fig. 2d) and 50 mg/kg MCL almost restored the normal myocardial architecture except for some cell vacuolization that still could be detected (Fig. 2e).

Cardiac Function

As observed in Table 4, heart rate (HR) was roughly the same among all study groups. By contrast, cardiac output (CO) and stroke volume (SV) were declined from 66.2 ± 5.9 ml/min and 2.31 ± 0.24 ml/beat in sham group to 41.8 ± 5.2 ml/min and 1.82 ± 0.15 ml/beat in control DOX mice, respectively ($P < 0.05$). Slight elevations in CO values (59.2 ± 3.9) were observed in DOX mice treated with 50 mg/kg MCL that was not statistically significant. SV was the only cardiac function indicator that increased significantly after treatment with 50 mg/kg MCL in DOX mice as compared to control DOX group (2.19 ± 0.22, $P < 0.05$) (Table 4).

PI3K/Akt Signaling Pathway

The chief members of the PI3K/Akt signaling pathway, i.e., PI3K, p-Akt, and p-PTEN proteins were measured in the cardiac tissues of all study groups. While PI3K and p-Akt levels had significantly been elevated in the DOX mice, the levels of p-PTEN were declined in the same control DOX animals ($P < 0.01$). 25 mg/kg and 50 mg/kg doses of MCL dose-dependently attenuated cardiac PI3K levels and elevated p-PTEN levels in heart ($P < 0.01$). In case of p-Akt, only 50 mg/kg MCL significantly reduced its cardiac levels ($P < 0.05$) (Fig. 3). We additionally evaluated tissue levels of p-Bad and caspase-3 levels, and found highly elevated levels of these proteins in the control DOX-treated mice ($P < 0.01$). In addition to p-Bad levels, the cardiac caspase-3 levels were dose-dependently reduced in DOX mice receiving 25 mg/kg and 50 mg/kg MCL ($P < 0.05$, $P < 0.01$. respectively) (Fig. 3). MCL had no significant effect on the cardiac levels of PI3K, p-Akt, p-PTEN, p-Bad, and caspase-3 in healthy mice (Fig. 3).

Discussion

Natural sesquiterpene lactones activate nicotinamide adenine dinucleotide (NADP) oxidases with recognized anti-inflammatory and anti-cancer properties and therefore are known to possess protective actions against various conditions like immune disorders [14], Alzheimer [15], hepatic fibrosis [16], and gastric cancer [17].

PI3K/Akt is a critical signaling pathway involved in the regulation of programmed cell death, i.e., apoptosis [18] that after activation leads to increased levels of anti-apoptotic

Table 3 Serum markers of cardiac injury

	Sham ($N=6$)	DOX ($N=6$)	DOX + 12.5 MCL ($N=6$)	DOX + 25 MCL ($N=6$)	DOX + 50 MCL ($N=6$)	MCL 50 ($N=6$)
MYO (ng/ml)	2.63 ± 0.88	5.37 ± 1.24[a]	5.41 ± 0.95[a]	5.32 ± 1.06[a]	5.45 ± 1.12[a]	2.55 ± 0.75
H-FABP (ng/ml)	3.85 ± 1.33	7.41 ± 1.62[a]	7.47 ± 1.35[a]	7.30 ± 1.48[a]	6.91 ± 1.24[a]	3.97 ± 1.09
GP-BB (ng/ml)	34.7 ± 6.81	51.9 ± 8.22[a]	49.2 ± 7.16[a]	52.8 ± 6.73[a]	42.85 ± 7.23[a]	36.1 ± 4.21
CK-MB (U/L)	7.24 ± 1.65	22.73 ± 2.78[a]	20.84 ± 2.69[a]	17.42 ± 2.11[a]	14.39 ± 2.61[a,b]	6.95 ± 1.78
cTnI (ng/ml)	3.28 ± 0.95	6.77 ± 1.18[a]	6.32 ± 1.25[a]	5.47 ± 0.95[a]	4.66 ± 0.83[a,b]	2.81 ± 0.86

Sham, healthy control mice; DOX, DOX-induced cardiotoxic control mice; DOX + 12.5 MCL, DOX-induced cardiotoxic mice treated with 12.5 mg/kg MCL; DOX + 25 MCL, DOX-induced cardiotoxic mice treated with 25 mg/kg MCL; DOX + 50 MCL, DOX-induced cardiotoxic mice treated with 50 mg/kg MCL; MCL 50 ($N=6$), healthy mice receiving 50 mg/kg MCL. Values are presented as mean ± SD

CK-MB creatine kinase MB, *cTnI* cardiac troponin I, *DOX* doxorubicin, *GP-BB* glycogen phosphorylase BB, *H-FABP* heart-type fatty acid-binding protein, *MCL* micheliolide, *MYO* myoglobin

[a] $P < 0.05$ versus Sham

[b] $P < 0.05$ versus DOX

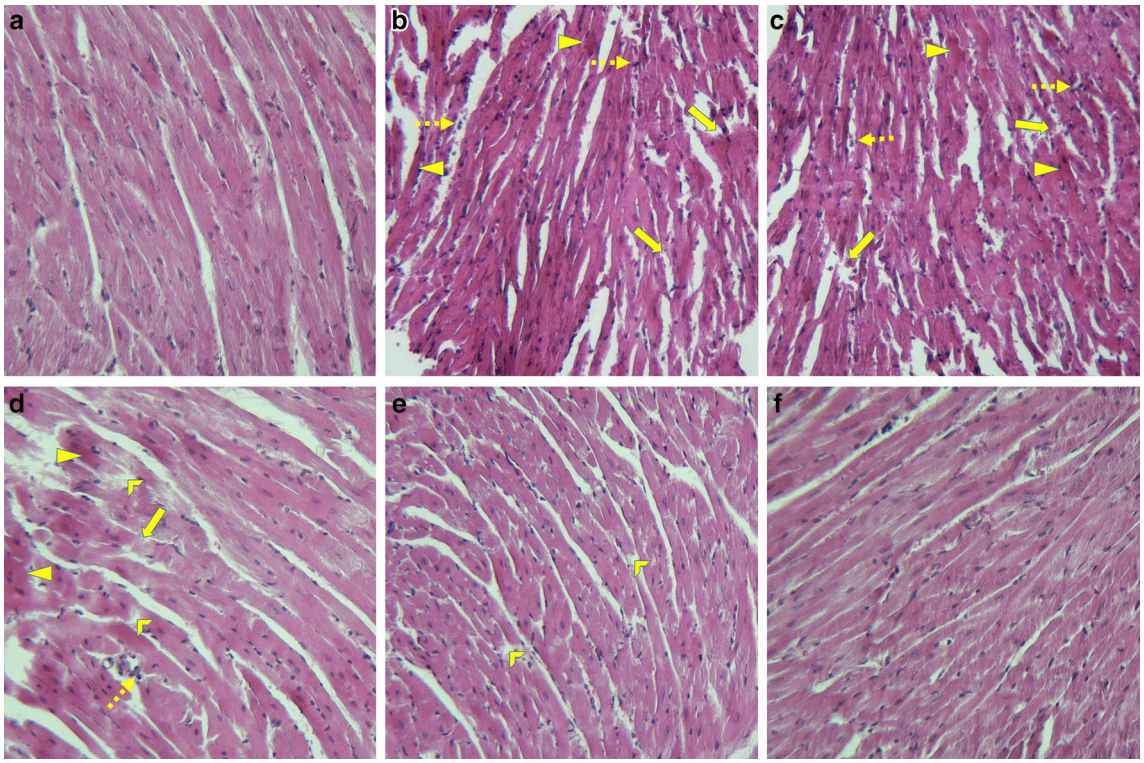

Fig. 2 Effects of MCL on cardiac histopathology. Healthy control mice ($N=6$) (**a**), DOX-induced cardiotoxic control mice ($N=6$) (**b**), DOX-induced cardiotoxic mice treated with 12.5 mg/kg MCL ($N=6$) (**c**), DOX-induced cardiotoxic mice treated with 25 mg/kg MCL ($N=6$) (**d**), DOX-induced cardiotoxic mice treated with 50 mg/kg MCL ($N=6$) (**e**); healthy mice receiving 50 mg/kg MCL ($N=6$) (**g**). Cardiac sections have been stained with hematoxylin and eosin

Table 4 Indices of cardiac function

	Sham ($N=6$)	DOX ($N=6$)	DOX + 12.5 MCL ($N=6$)	DOX + 25 MCL ($N=6$)	DOX + 50 MCL ($N=6$)	MCL 50 ($N=6$)
HR (beats/min)	252 ± 26	248 ± 31	244 ± 28	251 ± 24	243 ± 21	260 ± 25
CO (ml/min)	66.2 ± 5.9	41.8 ± 5.2[a]	44.1 ± 3.3[a]	53.6 ± 4.7[a]	59.2 ± 3.9[a]	62.2 ± 4.8
SV (ml/beat)	2.31 ± 0.24	1.82 ± 0.15[a]	1.88 ± 0.21[a]	2.04 ± 0.18[a]	2.19 ± 0.22[a,b]	2.43 ± 0.27

Sham, healthy control mice; DOX, DOX-induced cardiotoxic control mice; DOX + 12.5 MCL, DOX-induced cardiotoxic mice treated with 12.5 mg/kg MCL; DOX + 25 MCL, DOX-induced cardiotoxic mice treated with 25 mg/kg MCL; DOX + 50 MCL, DOX-induced cardiotoxic mice treated with 50 mg/kg MCL; MCL 50 ($N=6$), healthy mice receiving 50 mg/kg MCL. Values are presented as mean ± SD

CO cardiac output, *DOX* doxorubicin, *HR* heart rate, *MCL* micheliolide, *SV* stroke volume

[a] $P < 0.05$ versus Sham

[b] $P < 0.05$ versus DOX

proteins and thereby eliminates damaged cells with minimal local inflammation [19]. In the present study, we found that mice in DOX group had elevated levels of cardiac PI3K and Akt, the main components of the PI3K/Akt signaling pathway; moreover, cardiac levels of p-PTEN, the inhibitor of PI3K/Akt signaling pathway, had significantly been decreased. Treatment with MCL decreased PI3K and Akt levels and simultaneously increased p-PTEN levels in the heart tissues of DOX mice. By contrast, Yu et al. reported reduced levels of p-PI3K, p-Akt, and p-mTOR in the cardiac tissues of DOX-treated mice and that 2-week treatment with apigenin, a natural flavonoid, elevated their levels [20]. Similar reductions in the cardiac levels of cardiac p-Akt in mice have been reported by Cao et al. who found protective potential of astragalus polysaccharide against DOX-induced cardiotoxicity [21]. This contrariwise observation could be explained by the fact that the cardiac levels of both Bad and p-Bad, a salient pro-apoptotic protein [22], as well as

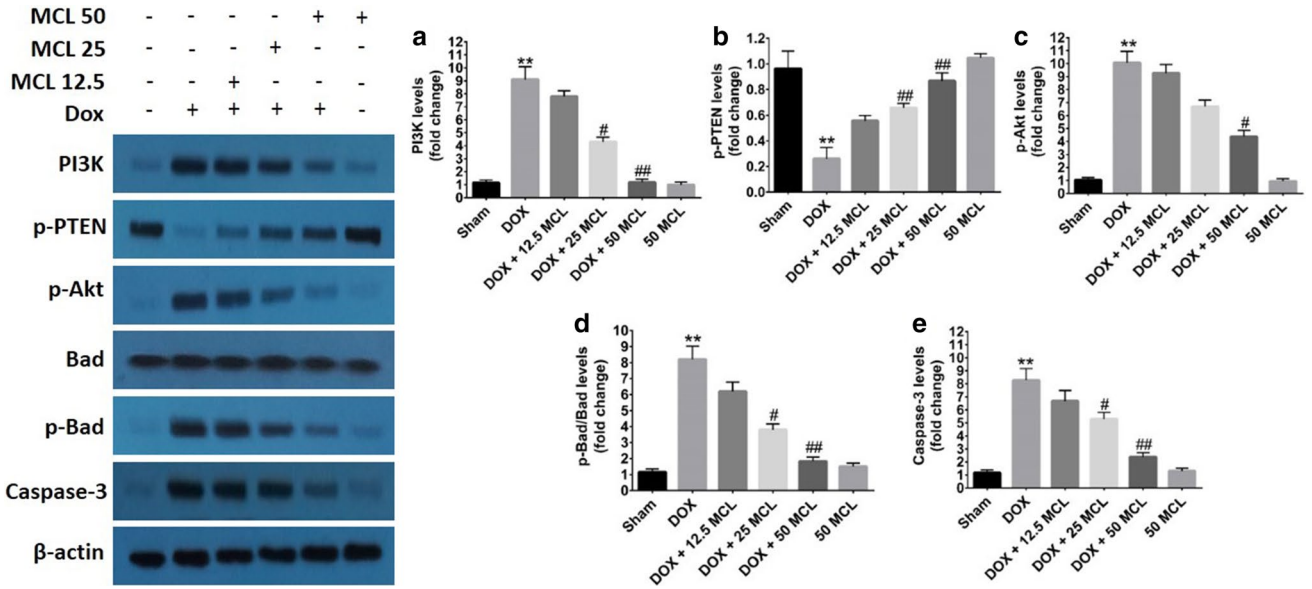

Fig. 3 Effects of MCL on cardiac levels of PI3K (**a**), p-PTEN (**b**), p-Akt (**c**), p-Bad/Bad (**d**), and caspase-3 (**e**) in DOX-induced cardiotoxic mice as evaluated by Western blotting. MCL, micheliolide; DOX, doxorubicin. Sham ($N=6$), healthy control mice; DOX ($N=6$), DOX-induced cardiotoxic control mice; DOX + 12.5 MCL ($N=6$), DOX-induced cardiotoxic mice treated with 12.5 mg/kg MCL; DOX + 25 MCL ($N=6$), DOX-induced cardiotoxic mice treated with 25 mg/kg MCL; DOX + 50 MCL (N = 6), DOX-induced cardiotoxic mice treated with 50 mg/kg MCL; MCL 50 ($N=6$), healthy mice receiving 50 mg/kg MCL. *p < 0.05, **p < 0.01, ***p < 0.001 versus Sham. #p < 0.05, ##p < 0.01, ###p < 0.001 versus DOX

apoptotic marker caspase-3 levels [23] were identified to be elevated in the present investigation; since increased activities of PI3K/Akt signaling pathway is associated with anti-apoptotic sequels [18], the increased activities of the pathway was probably secondary in order to counteract the actions of apoptotic proteins; therefore, upon attenuations in Bad, p-Bad, and caspase-3 levels after treatment with MCL, the levels of PI3K and p-Akt were also declined.

NF-kB is a protein complex that controls transcription of pro-inflammatory cytokines and therefore, is known as the master regulator of inflammation [24]. Elevated activities of NF-kB p65 in the cardiac tissues of DOX mice were reduced after MCL treatment. Likewise, increased expressions of TNF-α and IL-1β were alleviated by MCL in DOX-treated mice. These are in line with the findings obtained by Guo et al. who report that DOX-related inflammation is mediated by NF-kB signaling pathway in H9c2 cardiac cells [25]. Some report that active Akt inhibits NF-κB activity in DOX-treated HEK293, MDA-MB-435s, and melanoma cancer cells [26–28]; nevertheless, these reports are clearly in contrast with our observations and the findings obtained by other mechanistic studies as it has been documented that Akt stimulates IKK (IκB kinase) activity by phosphorylation on T23 in the IKKα subunit. The IKK complex then phosphorylates both the IκB (inhibitor of κB) and the p65 subunit, enhancing the activities of NF-κB transcription factor [29, 30]. In addition to the direct activation of anti-apoptotic mediators, Akt seems to be involved in the inhibition of NF-κB signaling pathway according to in vitro studies conducted on DOX-treated HEK293, MDA-MB-435s, and melanoma cancer lines [26–28]; these findings are clearly in contrast with our results. Nevertheless, this contradiction could be justified by the different in vivo nature of the present investigation conducted on healthy cardiac tissues of mice rather than malignant cells.

Increased production of reactive oxygen species (ROS) in DOX-induced cardiotoxicity is a major contributing factor for the deterioration of cardiomyocyte disintegration and cardiac function [31]. Recently investigated protective agents against DOX-induced cardiotoxicity, i.e., enoxaparin and nicorandil have been shown to successfully attenuate oxidative stress [32, 33]. We, similarly, demonstrated the anti-oxidative stress properties of MCL in DOX-induced cardiotoxicity in mice as the cardiac levels of MDA were reduced and the cardiac activities of SOD and GPX together with gene expressions of the anti-oxidant proteins HO-1 and NQO-1 were increased dose-dependently.

H-FABP, GP-BB, and myoglobin are sensitive markers of cardiomyocyte damage in the serum [34–36]. While increased levels of H-FABP, GP-BB, and myoglobin were observed in the serum of DOX-induced cardiotoxic mice, MCL only slightly reduced H-FABP and GP-BB levels and had no effect on the serum levels of myoglobin. Despite being sensitive cardiac injury markers, these agents have mainly been studied on myocardial infarction; Doxorubicin, however, is a toxic agent that impairs the skeletal muscles

[37], brain and spinal cord [38], liver [39], and adipocytes [40]; and because of the wide range of tissue damage, the inability of MCL in reducing their concentrations could probably be justified. Conversely, MCL dose-dependently reduced the serum cTnI and CK-MB levels. This could be a precious finding when we remind that both cTnI and CK-MB are mainly found in the cardiac tissues [41, 42]. To better elucidate the potential protective effects of MCL in DOX-induced cardiotoxic mice, we examined the histopathology of the cardiac tissues as well as cardiac functions across the study groups. Dose-dependent improvements both in tissue indices of inflammation/necrosis and cardiac function supported the observed reductions of CK-MB and cTnI in the serum of mice.

In conclusion, our findings underline the protective actions of MCL against DOX-induced cardiotoxicity in mice via repressing PI3K/Akt/NF-kB signaling pathway by reducing the serum markers of cardiac injury CK-MB and cTnI, improving the indices of cardiac function, i.e., cardiac output and stroke volume, ameliorating the tissue indicators of inflammation and necrosis.

Acknowledgements This work was supported by the grant from the Student Research Committee, Tabriz University of Medical Sciences.

Compliance with Ethical Standards

Conflict of interest The authors declare that they have no conflict of interest.

References

1. McGowan, J. V., Chung, R., Maulik, A., Piotrowska, I., Walker, J. M., & Yellon, D. M. (2017). Anthracycline chemotherapy and cardiotoxicity. *Cardiovascular Drugs and Therapy, 31*, 63–75.
2. Rahman, A. M., Yusuf, S. W., & Ewer, M. S. (2007). Anthracycline-induced cardiotoxicity and the cardiac-sparing effect of liposomal formulation. *International Journal of Nanomedicine, 2*, 567.
3. Volkova, M., & Russell, R. (2011). Anthracycline cardiotoxicity: Prevalence, pathogenesis and treatment. *Current Cardiology Reviews, 7*, 214–220.
4. de Oliveira Silva, J., Miranda, S. E. M., Leite, E. A., de Paula Sabino, A., Borges, K. B. G., Cardoso, V. N., Cassali, G. D., Guimarães, A. G., Oliveira, M. C., & de Barros, A. L. B. (2018). Toxicological study of a new doxorubicin-loaded pH-sensitive liposome: A preclinical approach. *Toxicology and Applied Pharmacology, 352*, 162–169
5. Renu, K., Abilash, V., Pichiah, P. T., & Arunachalam, S. (2017). Molecular mechanism of doxorubicin-induced cardiomyopathy: An update. *European Journal of Pharmacology, 818*, 241–253
6. De Angelis, A., Urbanek, K., Cappetta, D., Piegari, E., Ciuffreda, L. P., Rivellino, A., Russo, R., Esposito, G., Rossi, F., & Berrino, L. (2016). Doxorubicin cardiotoxicity and target cells: A broader perspective. *Cardio-Oncology, 2*, 2.
7. Viennois, E., Xiao, B., Ayyadurai, S., Wang, L., Wang, P. G., Zhang, Q., Chen, Y., & Merlin, D. (2014). Micheliolide, a new sesquiterpene lactone that inhibits intestinal inflammation and colitis-associated cancer. *Laboratory Investigation, 94*, 950.
8. Sun, Z., Li, G., Tong, T., & Chen, J. (2017). Micheliolide suppresses LPS-induced neuroinflammatory responses. *PLoS ONE, 12*, e0186592.
9. Zhang, Q., Jiang, X., He, W., Wei, K., Sun, J., Qin, X., Zheng, Y., & Jiang, X. (2017). MCL plays an anti-inflammatory role in mycobacterium tuberculosis-induced immune response by inhibiting NF-κB and NLRP3 inflammasome activation. *Mediators of Inflammation*. https://doi.org/10.1155/2017/2432904.
10. Zhong, J., Gong, W., Chen, J., Qing, Y., Wu, S., Li, H., Huang, C., Chen, Y., Wang, Y., & Xu, Z. (2018). Micheliolide alleviates hepatic steatosis in db/db mice by inhibiting inflammation and promoting autophagy via PPAR-γ-mediated NF-κB and AMPK/mTOR signaling. *International Immunopharmacology, 59*, 197–208.
11. Montgomery, M. D., Chan, T., Swigart, P. M., Myagmar, B., Dash, R., & Simpson, P. C. (2017). An alpha-1A adrenergic receptor agonist prevents acute doxorubicin cardiomyopathy in male mice. *PLoS ONE, 12*, e0168409.
12. Mantawy, E. M., El-Bakly, W. M., Esmat, A., Badr, A. M., & El-Demerdash, E. (2014). Chrysin alleviates acute doxorubicin cardiotoxicity in rats via suppression of oxidative stress, inflammation and apoptosis. *European Journal of Pharmacology, 728*, 107–118.
13. Govender, J., Loos, B., Marais, E., & Engelbrecht, A.-M. (2018). Melatonin improves cardiac and mitochondrial function during doxorubicin-induced cardiotoxicity: A possible role for peroxisome proliferator-activated receptor gamma coactivator 1-alpha and sirtuin activity? *Toxicology and Applied Pharmacology, 358*, 86–101
14. Zhu, Z., Zhao, Y., Huo, H., Gao, X., Zheng, J., Li, J., & Tu, P. (2016). HHX-5, a derivative of sesquiterpene from Chinese agarwood, suppresses innate and adaptive immunity via inhibiting STAT signaling pathways. *European Journal of Pharmacology, 791*, 412–423.
15. Amoah, S. K., Dalla Vecchia, M. T., Pedrini, B., Carnhelutti, G. L., Gonçalves, A. E., dos Santos, D. A., Biavatti, M. W., & de Souza, M. M. (2015). Inhibitory effect of sesquiterpene lactones and the sesquiterpene alcohol aromadendrane-4β, 10α-diol on memory impairment in a mouse model of Alzheimer. *European Journal of Pharmacology, 769*, 195–202.
16. Lai, L., Chen, Y., Tian, X., Li, X., Zhang, X., Lei, J., Bi, Y., Fang, B., & Song, X. (2015). Artesunate alleviates hepatic fibrosis induced by multiple pathogenic factors and inflammation through the inhibition of LPS/TLR4/NF-κB signaling pathway in rats. *European Journal of Pharmacology, 765*, 234–241.
17. Zhang, X.-W., Wang, S., Tu, P.-F., & Zeng, K.-W. (2018). Sesquiterpene lactone from Artemisia argyi induces gastric carcinoma cell apoptosis via activating NADPH oxidase/reactive oxygen species/mitochondrial pathway. *European Journal of Pharmacology, 837*, 164–170
18. Zhuang, Z., Zhao, X., Wu, Y., Huang, R., Zhu, L., Zhang, Y., & Shi, J. (2011). The anti-apoptotic effect of PI3K-Akt signaling pathway after subarachnoid hemorrhage in rats. *Annals of Clinical & Laboratory Science, 41*, 364–372.
19. Kitamura, Y., Koide, M., Akakabe, Y., Matsuo, K., Shimoda, Y., Soma, Y., Ogata, T., Ueyama, T., Matoba, S., & Yamada, H. (2014). Manipulation of cardiac phosphatidylinositol 3-kinase (PI3K)/Akt signaling by apoptosis regulator through modulating IAP expression (ARIA) regulates cardiomyocyte death during doxorubicin-induced cardiomyopathy. *Journal of Biological Chemistry, 289*, 2788–2800.
20. Yu, W., Sun, H., Zha, W., Cui, W., Xu, L., Min, Q., & Wu, J. (2017). Apigenin attenuates adriamycin-induced cardiomyocyte apoptosis via the PI3K/AKT/mTOR pathway. *Evidence-Based*

Complementary and Alternative Medicine. https://doi.org/10.1155/2017/2590676
21. Cao, Y., Ruan, Y., Shen, T., Huang, X., Li, M., Yu, W., Zhu, Y., Man, Y., Wang, S., & Li, J. (2014). Astragalus polysaccharide suppresses doxorubicin-induced cardiotoxicity by regulating the PI3k/Akt and p38MAPK pathways. *Oxidative Medicine and Cellular Longevity*. https://doi.org/10.1155/2014/674219
22. Virdee, K., Parone, P., & Tolkovsky, A. (2000). Phosphorylation of the pro-apoptotic protein BAD on serine 155, a novel site, contributes to cell survival. *Current Biology, 10*, 1151–1154.
23. Wolf, B. B., Schuler, M., Echeverri, F., & Green, D. R. (1999). Caspase-3 is the primary activator of apoptotic DNA fragmentation via DNA fragmentation factor-45/inhibitor of caspase-activated DNase inactivation. *Journal of Biological Chemistry, 274*, 30651–30656.
24. Liu, T., Zhang, L., Joo, D., & Sun, S.-C. (2017). NF-κB signaling in inflammation. *Signal Transduction and Targeted Therapy, 2*, 17023.
25. Guo, R.-M., Xu, W.-M., Lin, J.-C., Mo, L.-Q., Hua, X.-X., Chen, P.-X., Wu, K., Zheng, D.-D., & Feng, J.-Q. (2013). Activation of the p38 MAPK/NF-κB pathway contributes to doxorubicin-induced inflammation and cytotoxicity in H9c2 cardiac cells. *Molecular Medicine Reports, 8*, 603–608.
26. Ho, W. C., Dickson, K. M., & Barker, P. A. (2005). Nuclear factor-κB induced by doxorubicin is deficient in phosphorylation and acetylation and represses nuclear factor-κB-dependent transcription in cancer cells. *Cancer Research, 65*, 4273–4281.
27. Sims, J. T., Ganguly, S. S., Bennett, H., Friend, J. W., Tepe, J., & Plattner, R. (2013). Imatinib reverses doxorubicin resistance by affecting activation of STAT3-dependent NF-κB and HSP27/p38/AKT pathways and by inhibiting ABCB1. *PLoS ONE, 8*, e55509.
28. Romano, M. F., Avellino, R., Petrella, A., Bisogni, R., Romano, S., & Venuta, S. (2004). Rapamycin inhibits doxorubicin-induced NF-κB/Rel nuclear activity and enhances the apoptosis of melanoma cells. *European Journal of Cancer, 40*, 2829–2836.
29. Bai, D., Ueno, L., & Vogt, P. K. (2009). Akt-mediated regulation of NFκB and the essentialness of NFκB for the oncogenicity of PI3K and Akt. *International journal of cancer, 125*, 2863–2870.
30. Balwani, S., Chaudhuri, R., Nandi, D., Jaisankar, P., Agrawal, A., & Ghosh, B. (2012). Regulation of NF-κB activation through a novel PI-3K-independent and PKA/Akt-dependent pathway in human umbilical vein endothelial cells. *PLoS ONE, 7*, e46528.
31. Cappetta, D., De Angelis, A., Sapio, L., Prezioso, L., Illiano, M., Quaini, F., Rossi, F., Berrino, L., Naviglio, S., & Urbanek, K. (2017). Oxidative stress and cellular response to doxorubicin: A common factor in the complex milieu of anthracycline cardiotoxicity. *Oxidative Medicine and Cellular Longevity*. https://doi.org/10.1155/2017/1521020
32. Shaker, R. A., Abboud, S. H., Assad, H. C., & Hadi, N. (2018). Enoxaparin attenuates doxorubicin induced cardiotoxicity in rats via interfering with oxidative stress, inflammation and apoptosis. *BMC Pharmacology and Toxicology, 19*, 3.
33. Asensio-López, M. C., Soler, F., Pascual-Figal, D., Fernández-Belda, F., & Lax, A. (2017). Doxorubicin-induced oxidative stress: The protective effect of nicorandil on HL-1 cardiomyocytes. *PLoS ONE, 12*, e0172803.
34. Vupputuri, A., Sekhar, S., Krishnan, S., Venugopal, K., & Natarajan, K. (2015). Heart-type fatty acid-binding protein (H-FABP) as an early diagnostic biomarker in patients with acute chest pain. *Indian Heart Journal, 67*, 538–542.
35. Lippi, G., Mattiuzzi, C., Comelli, I., & Cervellin, G. (2013). Glycogen phosphorylase isoenzyme BB in the diagnosis of acute myocardial infarction: A meta-analysis. *Biochemia Medica, 23*, 78–82.
36. Mythili, S., & Malathi, N. (2015). Diagnostic markers of acute myocardial infarction. *Biomedical Reports, 3*, 743–748.
37. Van Norren, K., Van Helvoort, A., Argiles, J., Van Tuijl, S., Arts, K., Gorselink, M., Laviano, A., Kegler, D., Haagsman, H., & Van Der Beek, E. (2009). Direct effects of doxorubicin on skeletal muscle contribute to fatigue. *British Journal of Cancer, 100*, 311.
38. Tangpong, J., Miriyala, S., Noel, T., Sinthupibulyakit, C., Jungsuwadee, P., & Clair, D. S. (2011). Doxorubicin-induced central nervous system toxicity and protection by xanthone derivative of Garcinia mangostana. *Neuroscience, 175*, 292–299.
39. Kalender, Y., Yel, M., & Kalender, S. (2005). Doxorubicin hepatotoxicity and hepatic free radical metabolism in rats: The effects of vitamin E and catechin. *Toxicology, 209*, 39–45.
40. Batatinha, H., Souza, C., Lima, E., Alonso-Vale, M. I., Cruz, M., Da Cunha, R., Lira, F., & Rosa, J. (2014). Adipose tissue homeostasis is deeply disrupted by doxorubicin treatment. *Cancer & Metabolism, 2*, P5.
41. Wu, A. H., Panteghini, M., Apple, F., Christenson, R., Dati, F., & Mair, J. (1999). Biochemical markers of cardiac damage: From traditional enzymes to cardiac-specific proteins. *Scandinavian Journal of Clinical and Laboratory Investigation, 59*, 74–82.
42. Kemp, M., Donovan, J., Higham, H., & Hooper, J. (2004). Biochemical markers of myocardial injury. *British Journal of Anaesthesia, 93*, 63–73.